Nitrogen Concentration and Temperature Dependence of Ag/SiN/p^+-Si Resistive Switching Structure

Da Chen, *Shi-Hua Huang

Materials Physics Department, Zhejiang Normal University, Jinhua 321004, CHINA
**e-mail: huangshihua@zjnu.cn*

In this study, resistive switching behaviors of Ag/SiN/p^+-Si device were investigated by adjusting nitrogen concentration and layer thickness. The device with a nitrogen concentration of 50% and a thickness of 10 nm has a typical bipolar resistive switching behavior with a low forming voltage (~ 4 V), a high on/off ratio (~ 10^2), an excellent endurance (>10^2) and a long retention time (>10^5 s). According to *I–V* characteristics analyses, electric transports in both a high resistance state and a low resistance state are dominated by hot electron emission which is caused by the electron trapping and detrapping through immovable nitrogen-related traps. The temperature dependence of a resistive switching behavior not only illustrates the existence and importance of the traps, but also discovers a new phenomenon of the transition about the polar of a resistive switching method. Surely, more efforts need to be made for deeper understanding of the carrier transport in SiN thin films.

Keywords: silicon nitride, resistive random access memory, temperature dependence of resistive switching behavior.

УДК 621.311.

INTRODUCTION

Recently, resistive random access memories (RRAMs) based on various kinds of materials have attracted great interest for their potential applications in the next generation nonvolatile memories [1–7]. As early as 1982, the resistive switching (RS) behavior in silicon-based thin films was studied [8]. In recent years, many investigations about silicon-based RS memory have focused on the intrinsic amorphous Si and various doped Si-based thin films due to their compatibility with the standard complementary metal-oxide-semiconductor (CMOS) technology [9–13]. To be exact, Chang and colleagues investigated the resistive switching characteristics and mechanism in active SiO_x-based resistive switching memory [9]. Then, Kim and colleagues discovered and reported different sides of SiN-based RS memory. An obvious RS phenomenon in Ag/Si_3N_4/Al memory was observed in 2010 [10], and a fully transparent SiN-based memory cell was fabricated using ITO/SiN/ITO capacitor in 2012 [11].

In 2008, Jo and colleagues designed a nanoscale RS memory structure based on planar silicon, which shows the excellent potential of application for RRAM with high yield, fast programming speed, high on/off ratio, excellent endurance, long retention time, and multibit capability [14]. Hong and colleagues studied the effect of the work function difference between top and bottom electrodes on the resistive switching properties of SiN films [15].

Nitride-based RS memory is characterized by a low-voltage operation, a high thermal conductivity, good insulating properties, and a wide optical bandgap [16]. Moreover, there are a lot of nitride-related traps in silicon nitride, which may be more suitable for application in RRAMs among various Si-based RS materials [16]. In our previous work [1], the growth condition of a dielectric layer was studied by changing the sputtering atmosphere, growth temperature, sputtering power, sputtering time, etc. Therefore, we employed a similar method to study the effect of nitrogen concentration and layer thickness in SiN thin films. Then, we chose the device with the best RS properties among Ag/SiN/p^+-Si devices to investigate the conduction mechanism in a low resistance state (LRS) and a high resistance state (HRS). Finally, the temperature dependence of RS characteristics was investigated for a better understanding of a switching mechanism.

EXPERIMENTAL DETAILS

A single crystal silicon wafer with a thickness of ~ 300 μm and a resistivity of ~ 0.0015 Ω·cm was used as the substrate and the bottom electrode. The schematic diagram of the Ag/SiN/p^+-Si device is shown in Figure 1. After being cleaned by the standard RCA cleaning technology [17], a SiN thin film was deposited by a radio frequency (*RF*) reactive magnetron sputtering method. The base pressure of the vacuum chamber was better than 3.0×10^{-3} Pa. The deposition was implemented in the argon and nitrogen pressure of 1.0 Pa with the sputtering power of 100 W and the growth temperature of 500°C. During the sputtering, the total flow of the gases was 30 sc/cm, and argon and nitrogen worked as working gas and doped gas, respectively.

The deposition rate was about 2.0 nm per minute. Finally, Ag, the top electrode, was defined by depositing an Ag film (~ 500 nm) using a thermal evapo-

rator system through a shadow mask with a diameter of 1.0 mm to complete the full device structure. More information about the device is given in Table 1. The electrical measurement of the Ag/SiN/p^+-Si devices was performed using a digital sources tester (Keithley 2601), with the temperature range from 77 K to 300 K. During the electrical test, the bias voltage was applied on the top electrode while the bottom electrode was always grounded.

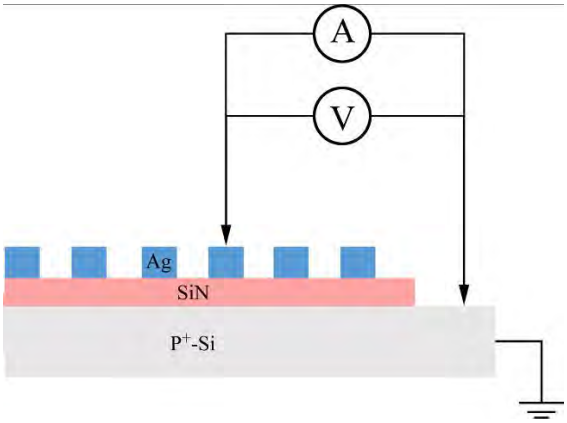

Fig. 1. Schematic diagram of Ag/SiN/p^+-Si device.

Table 1. Other deposition conditions for Ag/SiN/p^+-Si devices

Sample number	Nitrogen Content (N_2/Ar+N_2)	Layer Thickness (nm)
Sample 1	60%	20
Sample 2	50%	20
Sample 3	40%	20
Sample 4	30%	20
Sample 5	50%	10
Sample 6	50%	30

RESULTS AND DISCUSSIONS

Nitrogen concentration

Figure 2 shows the forming process (the insulating HRS changes into a stable reversible switching state) of devices with SiN thin films deposited at different nitrogen concentration. The forming voltage obviously increases with a higher nitrogen concentration. When the nitrogen concentration is up to 30% (N_2/(N_2+Ar)), the forming voltage is higher than 8 V. It is well known that a high forming voltage is harmful to devices because a complex external circuit is needed to be designed so as to protect devices. The inset in Fig. 2 shows the statistical distributions of the forming voltage for four devices. In order to illustrate the relative fluctuation of the forming voltage, we define a function (σ/μ), where σ is the standard deviation, μ the mean value. The values of σ/μ are 18.6%, 15.3%, 17.5%, 27.6% for Samples 1, 2, 3, and 4, respectively. Obviously, Sample 2 has the lowest values of the forming voltage and of σ/μ.

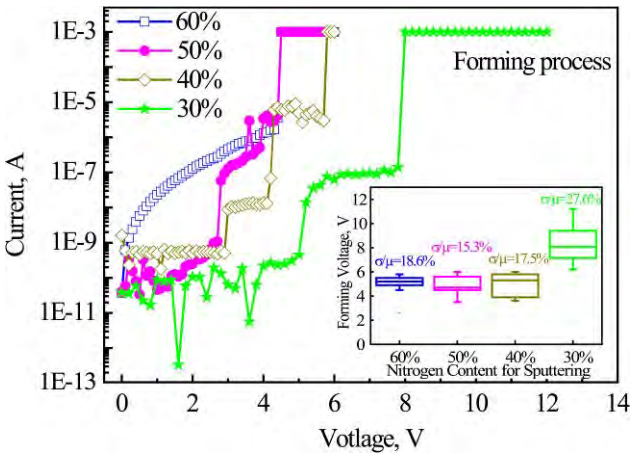

Fig. 2. Forming process of Ag/SiN/p^+-Si devices deposited at different radios of N_2/Ar: 12/18, 15/15, 18/12, and 21/9 for Samples 1, 2, 3 and 4, respectively. The inset shows the statistical distributions of the forming voltage for four devices.

During the electrical measurements, different devices with different nitrogen concentrations show different yields (a possibility for devices to have stable bipolar RS behaviors), and the result is shown in the inset in Figure 3. It is worth mentioning here that Sample 2 with a nitrogen concentration of 50% has the highest yield. In addition, we compare the RS behaviors of Samples 1, 2, 3 and 4 in the form of *I–V* curves. All the four devices show typical bipolar RS behaviors. The value of V_{SET} (the threshold voltage which transforms the device state from a HRS to a LRS) increases from 2.05 V to 4.58 V, with the nitrogen concentration decreasing from 60% to 30%. Also, the resistance in a LRS similarly increases from 883.6 Ω to 3497.6 Ω. During the endurance tests (not shown here), we found that Sample 2 with a nitrogen concentration of 50% can endure more than 100 stable DC voltage sweepings. Therefore, it is enough for us to assume that Sample 2 with a nitrogen concentration of 50% is worth being a subject for a deeper research among those four devices.

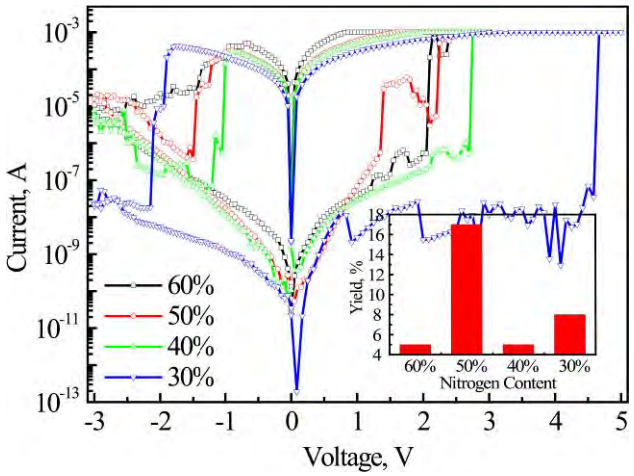

Fig. 3. Typical bipolar RS behaviors of Ag/SiN/p^+-Si devices with different nitrogen concentrations. The inset shows the yield of four devices.

Thickness of silicon nitride thin films

The thickness of SiN thin films plays an important role in RS behaviors [16]. Figure 4a shows a bipolar switching response for the three devices with different thicknesses of SiN thin films. With the thickness increasing from 10 nm to 30 nm, the V_{SET} increases from 1.85 V to 3.5 V and the V_{RESET} decreases from -0.63 V to -1.7 V. This is similar to the phenomenon of the $Ag/Si_3N_4/Al$ memory cells [16]. Kim and colleagues consider this phenomenon to be attributed to the increasing number of vacant traps for a thicker Si_3N_4 film. Endurance tests of three devices are shown in Figure 4b. The stability of resistance in a HRS and a LRS for Sample 5 is much better than that of Sample 2 or Sample 6. For Sample 2 and 6, the resistance in a HRS of both devices has a greater change after 60 switching cycles. The on/off ratio for the three devices is nearly 10^2, 10^3 and 10^1, respectively, and the retention time of Sample 2 is larger than 10^5 s. Afterwards, Fig. 4c is used to illustrate the statistical distributions of the resistance in a HRS and a LRS. From Fig. 4 it is clear that Sample 2 has the smallest fluctuation of resistance in a HRS and a LRS, when comparing the values of σ/μ among the three devices.

Among the investigated devices, Sample 2 shows the best RS behaviors. Consequently, Sample 2 was chosen to analyze the conduction mechanism, and the fitting analyses of *I–V* curves are shown in Figure 5. The slope of the fitting line in a LRS is about 0.899 as shown in Figure 5a. On the other hand, the experimental data of a HRS can be well fitted with the Schottky emission and the Poole-Frenkel emission as in Figure 5b. The slope is ~ 7.62 and ~ 4.93 for the two models when the bias voltage sweeps from 0 V to V_{SET}. Based on the Schottky emission and the Poole-Frenkel emission, a hopping process about the electron trapped in nitride-related traps is dominated due to the existence of a large number of nitride-related traps in SiN thin film [16]. When an electrical field is applied on the devices, a large number of electrons are injected from the bottom electrode into the SiN thin film. Then, electrons with enough energy jump over barriers, but some electrons get trapped by defects in the film. The difference of the $Ag/SiN/p^+$-Si device compared to the SiO_x-based memory device is in the conductive behavior in a LRS [9]. The conduction mechanism of the SiO_x-based memory device in a LRS invariably obeys the Ohmic law due to the continuous hopping between oxygen vacancies. Therefore, the Poole-Frenkel conduction mechanism is ascribed to the distribution of immovable nitride-related traps no matter with or without the help of an electric field.

Temperature dependence of SiN-based RS device

In order to understand the RS mechanism of the $Ag/SiN/p^+$-Si device, the temperature dependence of the RS behavior was investigated. During the cooling process, the $Ag/SiN/p^+$-Si device (Sample 5) had a traditional bipolar RS behavior at temperature above 205 K. But it switched from a bipolar mode into a unipolar mode at 205 K, as shown in Figure 6a. For a negative bias voltage sweeping (0 V to -2 V), the initial resistance state is a HRS, and the device switches to a LRS when the voltage is higher than -1.13 V. When the voltage sweeps back, the device has the reset process at -1 V, which is different from that at room temperature. The device needs more than two bias voltage sweepings to switch the resistance state successfully, and it still has a unipolar RS behavior in the negative bias if the measurement temperature is lower. The same phenomenon can also be observed in the low temperature electrical measurement of Samples 2 and 6, as shown in Figs. 6b and c, respectively. The transformation temperature is 210 K and 215 K for the two devices, respectively. So far, this phenomenon has not been reported, but we guess it is caused by an interior electric field in the SiN thin film.

Guan and colleagues inferred that the resistive switching behavior of the $ZrO_2/Au/ZrO_2$ structure is ascribed to the electron trapping and detrapping in nc-Au dispersed in ZrO_2, with an interior electric field built in the ZrO_2 layer [18]. However, the details and mechanism of the interior electric field have not been clear enough. Figure 7 shows the schematic diagram of the electrons transport behaviors for the $Ag/SiN/p^+$-Si memory device. When the negative bias voltage is applied on the Ag-TE in a low range, electrons are injected and trapped by the immovable nitrogen-related traps. Owing to high barriers in the interface between the SiN thin film and p^+-Si, few electrons could jump over the barriers to be collected by the bottom electrode, and the device stays in a HRS. When the nitrogen-related traps near the interface collect enough electrons and this part comes into a negative state, an interior electric field begins to be created. Then, the device does not turn into a LRS until the applied voltage counteracts the interior electric field, and the hopping conduction is dominated in the SiN thin film. In addition, a set process will happen if the applied voltage can not help the electrons pass through the interior electric field. This theory can explain this phenomenon well enough for Samples 5 and 2. But further studies need to be done to work out the problem of Sample 6.

Figure 8 shows the temperature dependence of resistance in a LRS and a HRS for the $Ag/SiN/p^+$-Si devices. It is clear that the resistance in a LRS

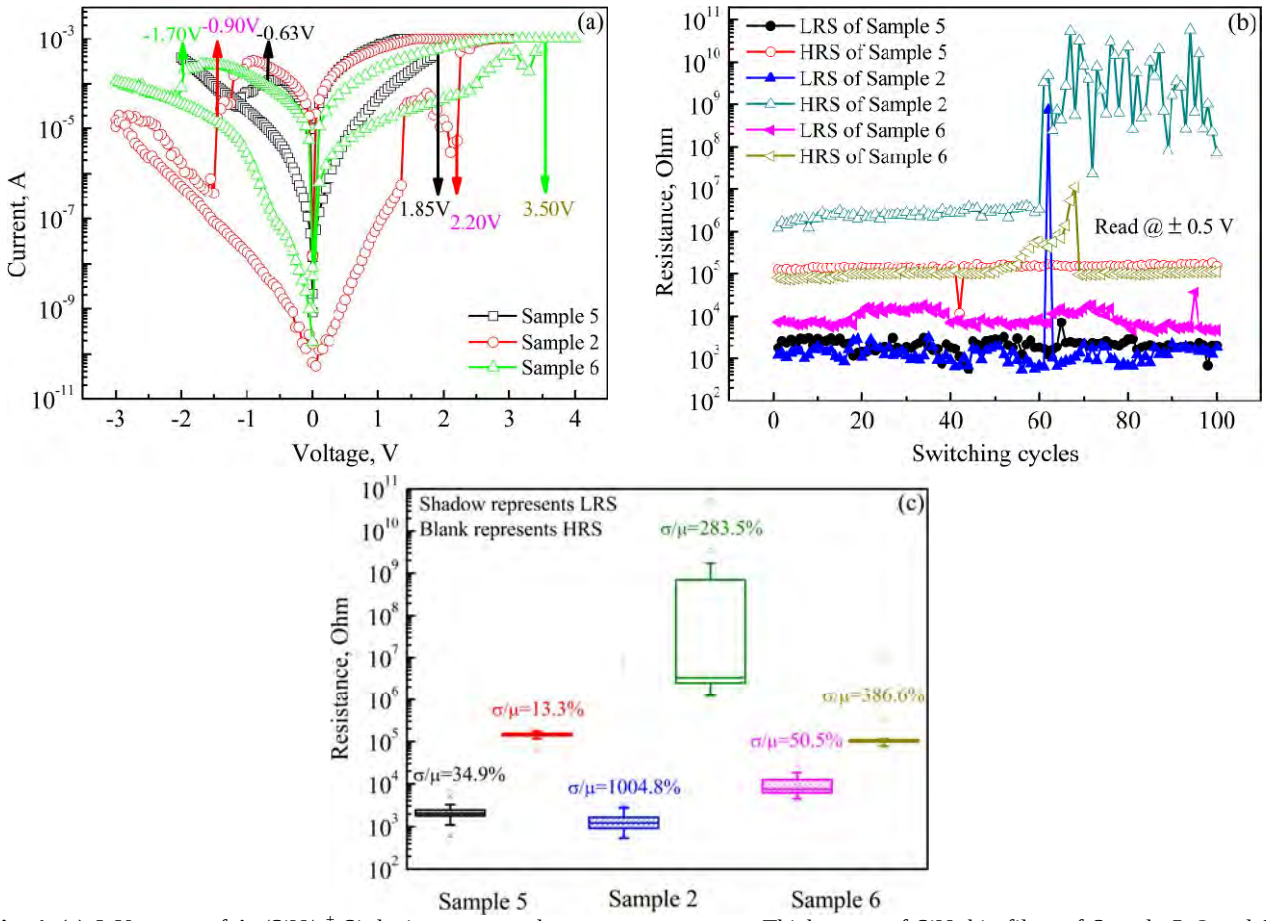

Fig. 4. (a) *I–V* curves of Ag/SiN/p^+-Si devices measured at room temperature. Thicknesses of SiN thin films of Sample 5, 2 and 6 deposited at the same atmosphere were 10 nm, 20 nm and 30 nm, respectively; (b) endurance characteristics of three devices; (c) statistical distributions of resistance in HRS and LRS for three devices.

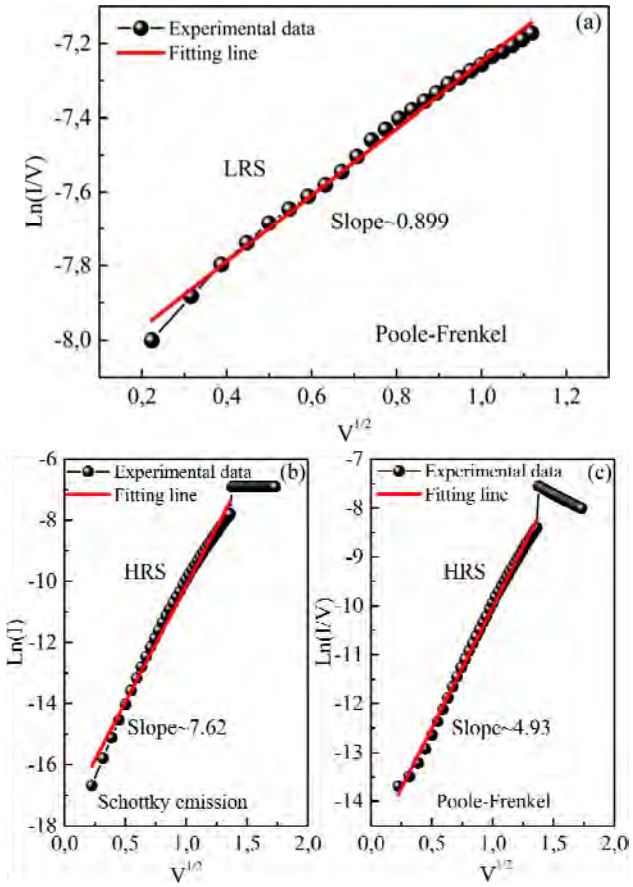

Fig. 5. (a) *I–V* curve for LRS of Sample 2 fitted by Poole-Frenkel at room temperature; *I–V* curve for HRS of Sample 2 fitted by (b) Schottky emission and (c) by Poole-Frenkel.

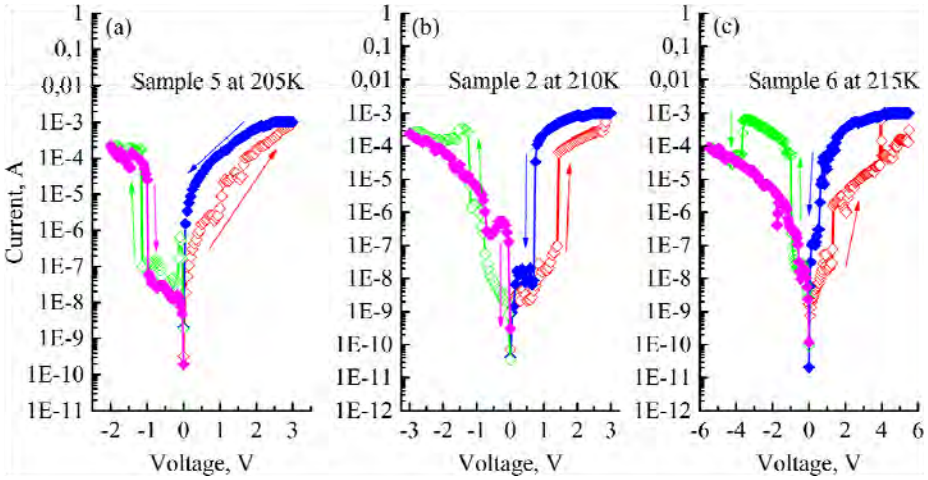

Fig. 6. *I–V* curves of Ag/SiN/p^+-Si devices in low temperature electrical measurement at 205 K, 210 K, and 215 K for Sample 5, 2, and 6, respectively.

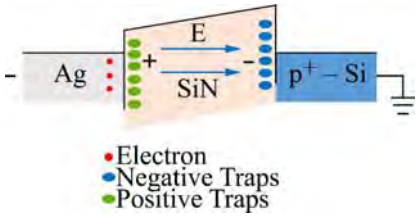

Fig. 7. Schematic diagram of electric transport behavior for Ag/SiN/p^+-Si device.

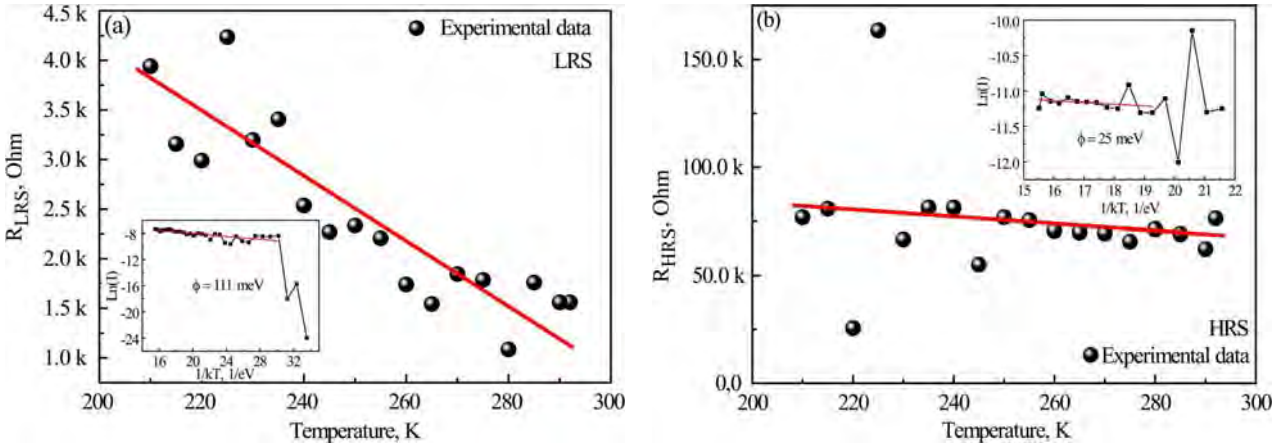

Fig. 8. Temperature dependence of resistance in (a) LRS and (b) HRS for Sample 5. Insets in Fig. 8 (a) and (b) are Arrhenius plots for the current-temperature curves measured in LRS and HRS, respectively.

decreases with the temperature raising and the relationship in a HRS between the resistance and temperature obeys the same law. This fitting line of the resistance decreasing with temperature strongly supports the idea that a semi-conduction is the dominant mechanism driven by nitrogen-related traps in the RS layer [19–20]. The temperature dependence of the current in a semiconductor is given by

$$I = I_0 \exp\left(\frac{-\phi_t}{kT}\right), \qquad (1)$$

where k is Boltzmann constant, ϕ_t the thermal activation energy and T the absolute temperature. ϕ_t can be extracted to be 111 meV and 25 meV from the slopes of the Arrhenius plots for a LRS and a HRS, as shown in the inset in Figs. 8a and b, respectively. From the analyses of the temperature dependence of the resistance in a HRS and a LRS, the hopping conduction based on the electron trapping and detrapping by nitrogen-related traps is dominated in a HRS and a LRS, and the barrier heights are 25 meV and 111 meV, respectively.

CONCLUSIONS

To sum up, we report the studies of the optimal nitrogen concentration and layer thickness of the Ag/SiN/p^+-Si devices fabricated by the RF reactive magnetic sputtering method. Based on the properties of typical RS behaviors, the device with a nitrogen concentration of 50% and a thickness of 10 nm shows an excellent potential of application in the RS memory device which has a low forming voltage (~ 4 V), a high on/off ratio (~ 10^2), an excellent endurance (>10^2), and a long retention time (>10^5 s).

For the conduction mechanism, the Schottky and the Poole-Frenkel emissions are the main behaviors for the electronic transport in a HRS. Also, Poole-Frenkel is still dominating in a LRS. Consequently, the switching mechanism of the Ag/SiN/p^+-Si device is attributed to the electron hopping based on the immovable nitrogen-related traps in the SiN thin film. Besides, the discovery of the transition from a bipolar mode to a unipolar mode at a low temperature is beneficial for deeper understanding of the physical mechanism of the carriers transport in the SiN thin films; however, more efforts need to be done to clear the blurry pictures.

ACKNOWLEDGEMENTS

This work was supported the Open Project Program of Surface Physics Laboratory (National Key Laboratory) of Fudan University (No. KF2015_02), the Open Project Program of National Laboratory for Infrared Physics, Chinese Academy of Sciences (No. M201503), Zhejiang Provincial Science and Technology Key Innovation Team (No. 2011R50012) and Zhejiang Provincial Key Laboratory (No. 2013E10022).

REFERENCES

1. Dong J., Huang S.H. *IEEE T. Nanotechnology*. 2014, **13**(3), 594–599.
2. Chen D., Huang S.H. *J Micro Nanolithogr MEMS MOEMS*. 2015, **14**(2), 024501–024501.
3. Liu H., Si M.W., Deng Y.X., Neal A.T., et al. *ACS Nano*. 2014, **8**(1), 1031–1038.
4. Shang J., Liu G., Yang H.L., Zhu X.J., et al. *Adv Funct Mater.* 2014, **24**(15), 2171–2179.
5. Hsu C.W., Chou L.J. *Nano Lett.* 2012, **12**(8), 4247–4253.
6. Chen J.Y., Hsin C.L., Huang C.W., Chiu C.H., et al. *Nano Lett.* 2013, **13**(8), 3671–3677.
7. Lu H., Kim D.J., Bark C.-W., Ryu S., et al. *Nano Lett.* 2012, **12**(12), 6289–6292.
8. Den B.W. *Appl. Phys. Lett*. 1982, **40**(9), 812–813.
9. Chang Y.F., Chen P.Y., Fowler B., Chen Y.T., et al. *J Appl Phys.* 2012, **112**(12), 123702–123709.
10. Kim H.D., An H.M., Kim K.C., Seo Y., et al. *Semicond Sci Technol.* 2010, **25**(6), 065002–065007.
11. Kim H.D., An H.M., Hong S.M., Kim T.G. *Phys Status Solidi A.* 2013, **210**(9), 1822–1827.
12. Waser R., Aono M. *Nat Mater.* 2007, **6**(11), 833–840.
13. Xia Q., Robinett W., Cumbie M.W., Banerjee N., et al. *Nano Lett.* 2009, **9**(10), 3640–3645.
14. Jo S.H., Lu W. *Nano Lett.* 2008, **8**(2), 392–397.
15. Hong S.M., Kim H.D., An H.M., Kim T.G. *IEEE Electron Devices Lett.* 2013, **34**(9), 1181–1183.
16. Zhu W., Zhang X., Fu X., Zhou Y., et al. *Phys Status Solidi A.* 2012. **209**(10), 1996–2001.
17. https://en.wikipedia.org/wiki/RCA_clean.
18. Guan W., Long S., Jia R., Liu M. *Appl Phys Lett.* 2007, **91**(6), 062111–062113.
19. Zhang Y., Deng N., Wu H., Yu Z., et al. *Appl Phys Lett.* 2014, **105**(6), 063508–063511.
20. Ren S., Ma Z.Y., Jiang X.F., Wang Y.F., et al. *Acta Phys. Sin.* 2014, **63**(16), 167201–167208.

Received 27.05.15
Accepted 07.09.15

Реферат

Поведение резистивного переключающего устройства на основе Ag/SiN/p^+-Si исследовали в условиях регулирования концентрации азота и толщины слоя. Устройство с концентрацией азота 50% и толщиной 10 нм имеет типичное биполярное поведение резистивного переключения с формированием низкого напряжения (~ 4 В), высокого отношение вкл/выкл (~ 10^2), отличная выносливость (> 10^2) и длительное время удерживания (> 10^5 с). В соответствии с анализами ВАХ, перенос электричества, как в состоянии высокого сопротивления, так и в состоянии низкого сопротивления обеспечивается при преобладании горячей эмиссии электронов, вследствие электронов захвата и их высвобождении на неподвижимых, связанных с азотом ловушек. Температурная зависимость поведения при резистивном переключении не только иллюстрирует существование и важность ловушек, но и обнаруживает новое явление перехода при использовании резистивного метода коммутации. Конечно, необходимы дополнительные усилия для более глубокого понимания переноса носителей заряда в тонких пленках SiN.

Ключевые слова: нитрид кремния, резистивная память с произвольным доступом, температурная зависимость резистивного поведения переключателей.